High-Capacity OFDMA Femtocells by Directional Antennas and Location Awareness

Ang-Hsun Tsai, *Student Member, IEEE,* Li-Chun Wang, *Fellow, IEEE,* Jane-Hwa Huang, *Member, IEEE,* and Ruey-Bing Hwang, *Senior Member, IEEE*

***Abstract*—In this paper, we propose a location-aware mechanism combined with a low-cost four-sector switched-beam directional antenna to enhance the spectrum efficiency of orthogonal frequency-division multiple access (OFDMA)-based femtocell systems. The considered location-awareness capability is specified in the current IEEE 802.16m WiMAX standard, but has not been applied to avoid the interference between indoor femtocells and outdoor macrocells. With the knowledge of the locations of outdoor users, the proposed four-sector switched-beam antenna in a femtocell can effectively avoid the interference among femtocells and macrocells by adjusting the number of OFDMA subcarriers used at each femtocell. Numerical results show that the proposed approach can significantly improve spectrum efficiency compared to the existing methods.**

***Index Terms*—Closed subscriber group (CSG), femtocell, four-sector switched-beam directional antenna, link reliability, location awareness, open subscriber group (OSG), orthogonal frequency-division multiple access (OFDMA), spectrum efficiency, two-tier interference.**

I. Introduction

FEMTOCELLS can improve system capacity and indoor coverage with low power and low cost [1]–[4]. Unlike base stations in conventional cellular systems, femtocells connect to the network center through the broadband wirelines inside the customers' homes. Due to short transmission distance, femtocells require very low transmission power. From the operator's viewpoint, deploying femtocells can also significantly improve system capacity because the same spectrum can be repeatedly used by a huge number of other femtocells. Femtocells can also off-load the traffic of the outdoor macrocell users toward the indoor femtocell base station (fBS). From the customers' perspective, the fBS is much closer than the outdoor macrocell base station (mBS), thereby improving indoor signal quality.

Manuscript received June 30, 2011; revised November 2, 2011; accepted November 7, 2011. Date of publication January 10, 2012; date of current version May 22, 2012. This work was supported in part by the National Science Council (NSC) of Taiwan, under Research Grant NSC 100-2221-E-009-103-MY3, and in part by the Industrial Technology Research Institute, Information and Communication Research Laboratories, Taiwan. Part of this work was presented at the IEEE Wireless Communications and Networking Conference, 2010.

A.-H. Tsai, L.-C. Wang, and R.-B. Hwang are with the Department of Electrical Engineering, National Chiao Tung University, Hsinchu 300, Taiwan (e-mail: anghsun@gmail.com; lichun@cc.nctu.edu.tw; raybeam@mail.nctu.edu.tw).

J.-H. Huang is with the Department of Electrical Engineering, National Chi Nan University, Nantou 545, Taiwan (e-mail: jhhuang@ncnu.edu.tw).

Color versions of one or more of the figures in this paper are available online at http://ieeexplore.ieee.org.

Digital Object Identifier 10.1109/JSYST.2011.2178724

However, the serious two-tier interference in femtocells is the key challenge [2]–[5]. After femtocells are densely deployed, both the femto-to-femto and the macro-to-femto interference occur. In the meanwhile, the macrocell users undergo the interference from the femtocells and macrocells as well. The severe two-tier interference significantly affects the system capacity because the subcarriers available for the femtocells are reduced.

In the literature, most studies on femtocells considered the omnidirectional femtocells and can be categorized into three kinds: power control, access method, and spectrum allocation.

In [1] and [6], the power control method for femtocells with omnidirectional antenna were discussed. In [1], an autoconfiguration method of transmit power was proposed for the code division multiple access (CDMA)-based femtocells with the shared spectrum allocation scheme. In [6], the authors proposed a distributed femtocell uplink power control to achieve higher signal-to-interference plus noise ratio performance on the condition that the link quality of the macrocell users can be guaranteed.

Access methods for femtocells were discussed in [3], [7], and [8]. In [3], the authors compared the closed subscriber group (CSG) and open subscriber group (OSG) femtocell systems, where the CSG fBSs only serve the authorized users, and the OSG fBSs can serve any users. Because the OSG users can select the base station with best signal quality among the femtocells and macrocells, the OSG scheme has better coverage than the CSG scheme. In [7], the authors studied different access methods for femtocells and proposed a hybrid access approach to improve the average throughput. In [8], the authors investigated the effects of access methods in the uplink femtocell systems. They suggested that the access method depend on the cellular user density in the time division multiple access/orthogonal frequency-division multiple access (OFDMA) network, and showed that open access is the optimal choice in the CDMA network.

In [9]–[14], spectrum allocation schemes for femtocells with omnidirectional antenna were discussed. In [9], the channel selection issues in the WiMAX-based femtocell systems was investigated by taking into account of the femto-to-femto interference. In [11], distributed channel selection schemes for femtocells were developed to improve the capacity by adjusting the number of used subcarriers. In [10], the authors analyzed the optimal fraction of spectrum allocated to macrocell and femtocell systems, in which the macrocell and femtocell systems are assigned with different frequency bands. In [12], the authors designed an on-demand two-tier resource allocation mechanism to improve the system throughput. In [13], the authors proposed the cognitive radio resource management scheme for femtocell networks to achieve the higher capacity with ensuring the delay requirement. Afterward, they further proposed the strategic game-based radio resource management scheme for femtocells to alleviate the severe femto-to-femto interference as well as improve the system capacity with the delay guarantee [14].

Fewer papers have examined the femtocell systems with directional antennas, such as [15]–[19]. Intuitively, directional antennas can increase signal strength due to higher antenna gain and decrease the interference due to the narrow-beam patterns. In [15], the uplink capacity in CDMA-based femtocell networks using sector antennas and time-hopping techniques were analyzed. The multiple antennas in CDMA-based femtocell systems were applied to reduce the unnecessary handover and enhance the indoor coverage [16]. However, the main focus of [15] and [16] was on the shared spectrum allocation scheme in the CDMA-based femtocell systems.

The receive antenna diversity was applied to mitigate the uplink co-channel interference and improve the signal reception quality for femtocells [17], [18]. In [19], the authors proposed power control method using switched parasitic array antenna in OFDMA-based femtocell networks to avoid the co-channel interference to macrocell users. Nevertheless, the works of [17]–[19] aimed to alleviate the co-channel interference by the antenna diversity. They did not investigate the impacts of the location of outdoor users and they also did not apply the partial usage of femtocell subcarriers approach to reduce the femto-to-macro interference. In our previous work [20], the capacity and link reliability of low-cost E-plane horns-based reconfigurable directional antenna for the OFDMA-based femtocell systems were investigated. The major research in [20] was to investigate the impact of directional antenna on the link reliability and capacity of indoor users. However, the impact of femtocells on outdoor users was not considered in [20].

In this paper, we develop a subcarrier number adjustment method combining with location-aware capability to mitigate the two-tier interference in OFDMA-based femtocell systems. We consider a four-sector switched-beam OFDMA-based femtocell system and utilize the location awareness capability in the IEEE 802.16m WiMAX system [21]. When an outdoor user is close to a femtocell, the number of occupied subcarriers is reduced to lower the interference. If an outdoor user is far away from the femtocells, the subcarriers can be fully utilized by the femtocell's users. We show that the proposed location-aware switched-beam femtocell system can improve its spectrum efficiency due to its capability of avoid interference to the outdoor users.

The remainder of this paper is organized as follows. Section II describes the system architecture, the proposed location awareness scheme, and the channel models. The major performance metrics are discussed in Section III. In Section IV, we compare radiation patterns of the four-sector switched-beam

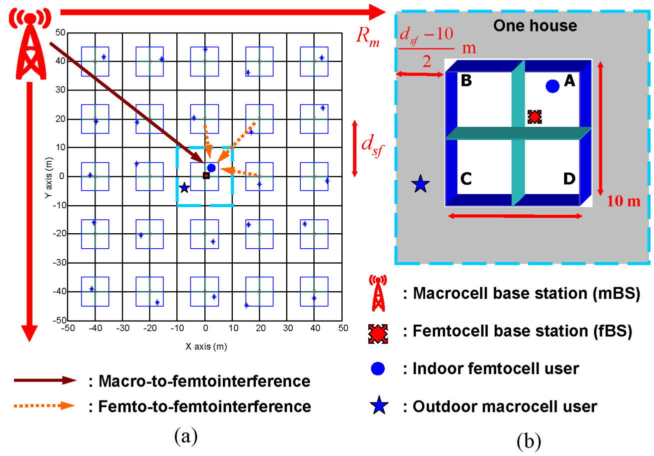

Fig. 1. Illustrative example of the two-tier inference scenario in femtocells. (a) Cluster of 25 femtocells, each of which faces femto-to-femto and macro-to-femto interference. (b) Each four-sector femtocell is surrounded by the streets with $(d_{\mathrm{sf}} - 10)/2$ m and one macrocell user is appeared in the street area of 25 femtocells.

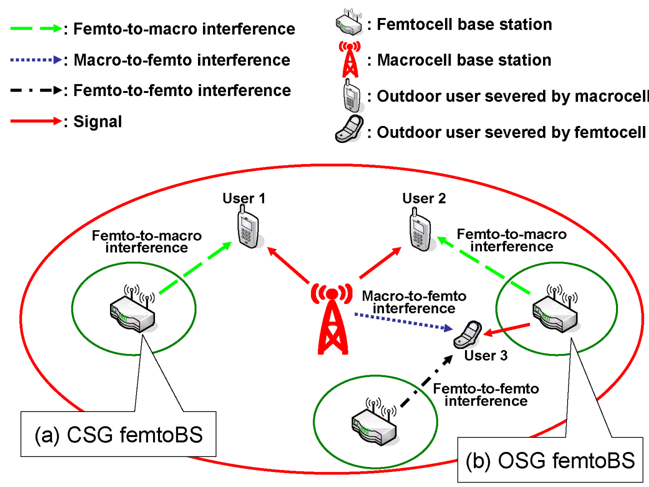

Fig. 2. Two-tier interference for outdoor users with two access methods. (a) CSG access method. (b) OSG access method.

directional antenna and the IEEE 802.16m sector antenna. We show the simulation results in Section V. Finally, our concluding remarks and future works are given in Section VI.

II. System Models

A. System Architecture

We consider the OFDMA-based femtocell systems in the campus or community environment. Fig. 1(a) shows a cluster of 25 femtocells and a macrocell with a radius of R_m m. Assume that each house covers an area of $100\,\mathrm{m}^2$ and has four $5 \times 5\,\mathrm{m}^2$ rooms. Let the fBS be deployed at the center of each house with a shift of (0.1 m, 0.1 m), and denote d_{sf} m as the separation distance between two neighboring fBSs. It is assumed that the femtocell user's locations are uniformly distributed within the house, and one outdoor user is located in the shadowed region with width of $(d_{\mathrm{sf}} - 10)/2$ m surrounding the house, as shown in Fig. 1(b).

Both the exclusive and shared spectrum allocation schemes in OFDMA-based femtocells are considered in our model. The former scheme allocates different frequency bands to the macrocell and femtocell system, and the later scheme allows the same spectrum shared by both the marcocell and femtocell system. Compared with the shared spectrum allocation schemes, the exclusive spectrum allocation scheme can reduce the mutual interference, but may have lower spectrum efficiency. On the contrary, the shared spectrum scheme can increase the spectrum efficiency at the cost of higher two-tier interference.

In the shared spectrum scheme, two spectrum management schemes are further considered and compared in this paper: CSG and OSG access methods. According to the CSG method, the outdoor macrocell user cannot access the femtocell. By contrast, if the OSG method is adopted, the macrocell users can access the femtocell. In principle, the CSG method can ensure privacy and security better than the OSG method. However, the interference issue of CSG is more severe than the OSG method because the outdoor user can be arranged to use the idle subcarriers of femtocells. Fig. 2 shows the two-tier interference scenario for an outdoor user in the OSG and CSG schemes.

B. Location Awareness

If the appearance of an outdoor macrocell user can be detected by the nearby femtocells, the usage of subcarriers in the femtocell system can be adjusted in order to reduce the interference to the macrocell system. Furthermore, location capability combined with network level signaling can support location-based services and emergency E911 calls. The locations of outdoor macrocell users can be estimated by many kinds of techniques, e.g., the network-managed, mobile station (MS)-managed, femtocell-assisted, and GPS-based methods [21]. For the network-managed location estimation method, the time of arrival and the angle of arrival in the uplink transmissions are used to locate the outdoor user. For the MS-managed method, a mobile user can calculate the location information with fewer interactions with the network compared with the network-managed location estimation method. The femtocell-assisted location determination method relies on mobile users which are not connected to any femtocells to collect the information of neighboring fBSs. Based on the collected information, the network can determine the macrocell user's location.

In the following, we discuss the subcarrier usage adjustment procedures to reduce interference for the location-aware femtocell systems. During the registration processes of femtocells, a cellular operator can obtain the location information of the femtocells [1], which is stored in the location database of femtocell gateways at the network center. After positioning an outdoor user, cellular networks inform the corresponding femtocell gateway to look up its location database, and notify the femtocells close to that particular outdoor user. By reducing the used subcarriers in femtocells, the link reliability of outdoor users can be ensured even with the shared spectrum allocation scheme. Location-aware femtocells need not reduce the subcarrier usage if an outdoor user is far away from them. By contrast, conventional femtocells without location awareness shall use fewer subcarriers to guarantee the link quality of the outdoor users. Hence, the location-aware femtocells can achieve higher femtocell capacity compared with the conventional femtocells. Usually, only the approximate location of the outdoor user is required by the location-aware femtocells to make decision about the subcarrier usage. If it is necessary to reduce more interference and estimate the macrocell user location more accurately, femtocell gateways can instruct more femtocells near that macrocell user to adjust subcarriers usage.

C. Channel Models

To evaluate the two-tier interference in the OFDMA-based hybrid macrocell and femtocell systems, we consider the following radio propagation effects, including path loss, wall penetration loss, shadowing, and frequency-selective multipath fading.

1) *Path Loss:* According to [22], the path loss between transmitter and receiver with the propagation distance d m is defined as

$$L(d)\,(\text{dB}) = \begin{cases} 20\log_{10}\left(\dfrac{4\pi d}{\lambda}\right), & d \le d_{\text{BP}} \\ 20\log_{10}\left(\dfrac{4\pi d_{\text{BP}}}{\lambda}\right) + 35\log_{10}\left(\dfrac{d}{d_{\text{BP}}}\right), & d > d_{\text{BP}} \end{cases} \tag{1}$$

where λ is the wavelength, d_{BP} is the break-point distance, and $d_{\text{BP}} = 5$ m and 30 m for indoor links and outdoor links at the 2.5 GHz carrier frequency, respectively.

2) *Wall Penetration Loss:* The wall penetration attenuation is assumed to be 5 dB per wall for indoor links, and 10 dB per wall for the outdoor-to-indoor links. We denote $\widetilde{\text{PL}}_i$ as the total penetration loss between the ith femtocell and the considered user, and $\widehat{\text{PL}}$ as the wall penetration loss between the macrocell and the considered user.

3) *Shadowing:* The log-normally distributed shadowing random variable $10^{\xi/10}$ is considered in our model, where ξ is a Gaussian-distributed random variable with zero mean. The shadowing standard deviations for the indoor links, the macrocell-to-femtocell links, and the femtocell-to-femtocell links are $\sigma = 5$ dB, 8 dB, and 10 dB, respectively.

4) *Frequency-Selective Multipath Fading:* To model the received link quality in the OFDMA system, the Stanford University interim-3 (SUI-3) channel model [23] is adopted in this paper. The SUI-3 channel model considers a three-tap channel with nonuniform delays.

III. Performance Metrics

In this paper, we consider the following performance metrics, including carrier to interference-and-noise ratio (CINR), link reliability, femtocell capacity, and spectrum efficiency.

A. Carrier to Interference-and-Noise Ratio

For the femtocell users, the two-tier interference comes from the macrocell and the other neighboring femtocells. Suppose that $\widehat{G}(\theta)$ is the antenna gain of the macrocell and $\widetilde{G}(\theta_i)$ is that of the ith femtocell. Due to the frequency selective fading, $|\widehat{H}_m|^2$ represents the link gain between the macrocell and the femtocell user, and $|\widetilde{H}_{i,m}|^2$ is that between the ith femtocell and the femtocell user. Therefore, the CINR of the mth subcarrier

TABLE I
MODULATION AND CODING SCHEMES

Modulation	Code Rate	Theoretical Spectrum Efficiency η (b/s/Hz)	Minimum CINR (dB)	EESM β (dB)
QPSK	1/2(4)	0.25	$\gamma_{\text{th}} = -2.5$ dB	2.18
QPSK	1/2(2)	0.5	0.5	2.28
QPSK	1/2	1	3.5	2.46
QPSK	3/4	1.5	6.5	2.56
16-QAM	1/2	2	9	7.45
16-QAM	3/4	3	12.5	8.93
64-QAM	1/2	3	14.5	11.31
64-QAM	2/3	4	16.5	13.8
64-QAM	3/4	4.5	18.5	14.71

QPSK: quadrature phase shift keying; QAM: quadrature amplitude modulation.

for the considered femtocell user is defined as

$$\gamma_{F,m} = \frac{\dfrac{\widetilde{P}_t \widetilde{G}(\theta_i) 10^{\frac{\tilde{\xi}_i}{10}} |\widetilde{H}_{i,m}|^2}{L(d_i)\widetilde{\text{PL}}_i}}{\dfrac{\widehat{P}_t \widehat{G}(\theta) 10^{\frac{\hat{\xi}}{10}} |\widehat{H}_m|^2}{L(D)\widehat{\text{PL}}} + \sum_{k=1,k\neq i}^{K} \dfrac{\widetilde{P}_t \widetilde{G}(\theta_k) 10^{\frac{\tilde{\xi}_k}{10}} |\widetilde{H}_{k,m}|^2}{L(d_k)\widetilde{\text{PL}}_k} + N_0} \quad (2)$$

where the first term of the denominator is the interference from the macrocell, and the second term is that from the neighboring femtocells. $\widehat{P}_t$ is the transmission power of macrocell and $\widetilde{P}_t$ is that of femtocells. $\widehat{\xi}$ is the shadowing between the macrocell and the femtocell user, and $\widetilde{\xi}_i$ is that between the ith femtocell and the considered femtocell user. D is the separation distance between the macrocell and the considered femtocell user. d_i is the separation distance from the ith femtocell to the considered femtocell user. N_0 is the noise power and K is the total number of femtocells.

For the macrocell users, the interference comes from all the adjacent femtocells. The CINR of the mth subcarrier for the considered macrocell user is expressed as

$$\gamma_{M,m} = \frac{\dfrac{\widehat{P}_t \widehat{G}(\theta) 10^{\frac{\hat{\xi}}{10}} |\widehat{H}_m|^2}{L(D)\widehat{\text{PL}}}}{\sum_{k=1}^{K} \dfrac{\widetilde{P}_t \widetilde{G}(\theta_k) 10^{\frac{\tilde{\xi}_k}{10}} |\widetilde{H}_{k,m}|^2}{L(d_k)\widetilde{\text{PL}}_k} + N_0}. \quad (3)$$

According to the exponential effective SIR mapping (EESM) method [24], we can map a vector of CINRs for multiple subcarriers to a single effective CINR. Suppose that the femtocell uses N_d subcarriers for transmission. The CINR for each subcarrier is γ_m, $m = 1, 2, \ldots, N_d$. Then, the effective CINRs for the N_d used subcarriers can be calculated by

$$\gamma_{\text{eff}}(\gamma_1, \gamma_2, ..., \gamma_{N_d}) = -\beta \cdot \ln\Big(\frac{1}{N_d} \sum_{m=1}^{N_d} \exp[-\gamma_m/\beta]\Big) \quad (4)$$

where β is the calibration factor for the selected modulation coding scheme (MCS) [24]. Table I lists the considered MCSs, the corresponding effective CINR thresholds, and the EESM parameter β. With the information of effective CINR, the MCS and the corresponding theoretical spectrum efficiency η can be determined according to Table I.

B. Link Reliability, Capacity, and Spectrum Efficiency

Link reliability P_{rel} is defined as the probability that the effective CINR of the considered user is higher than a predefined effective CINR threshold γ_{th}, that is

$$P_{\text{rel}} = \Pr[\gamma_{\text{eff}} \geq \gamma_{\text{th}}]. \quad (5)$$

Capacity in this paper is defined as the total throughput of an OFDMA-based femtocell. Consider that each femtocell uses N_d subcarriers for transmission. For bandwidth B, M-point fast Fourier transform (FFT), and the theoretical spectrum efficiency η, the corresponding an OFDMA system capacity can be calculated by

$$C = \frac{B}{M} \frac{N_d}{1+G} \cdot \eta \quad (6)$$

where G is the guard fraction defined in [25].

Next, we discuss the spectrum efficiency of femtocells with the exclusive and shared spectrum allocation schemes corresponding to 90% link reliability. In the exclusive spectrum scheme with the total bandwidth B, the femtocells and macrocells are allocated with nonoverlapping $B/2$ bandwidth. Denote C_{ex} as the femtocell capacity with link reliability $P_{\text{rel}} \geq 90\%$ for the required γ_{th}. In this case, the spectrum efficiency of one femtocell in the exclusive spectrum scheme is defined as

$$\text{SE}_{\text{ex}} = \frac{C_{\text{ex}}}{B}. \quad (7)$$

In the shared spectrum scheme, the femtocells use the same frequency band of bandwidth B as the macrocells. Let C_{sh} be the capacity of a femtocell with the link reliability $P_{\text{rel}} \geq 90\%$ for the required γ_{th}. Therefore, the spectrum efficiency for the shared spectrum scheme is defined as

$$\text{SE}_{\text{sh}} = \frac{C_{\text{sh}}}{B}. \quad (8)$$

Indeed, SE_{ex} and SE_{sh} defined in (7) and (8) are the measurements of spectrum efficiency improvement for one single femtocell. The spectrum efficiency SE_{ex} and SE_{sh} are for only one single femtocell. Although it is not equal to the spectrum efficiency of a heterogeneous macrocell/femtocell system, the considered spectrum efficiency can be used to quantitatively compare the spectrum efficiency of the exclusive and shared allocation schemes. Intuitively, with the two times of bandwidth, the exclusive spectrum allocation scheme may have less spectrum efficiency than the shared allocation scheme. However, in the shared spectrum scheme, femtocells must decrease the used subcarriers to ensure the link reliability of all the users, and thus significantly reduce the spectrum efficiency. Hence, we suggest exploiting the location awareness capability of the femtocell system to improve the spectrum efficiency of shared spectrum allocation scheme.

As discussed in Section II-B, the location-aware femtocell system can adaptively determine the number of subcarriers used by a femtocell depending on the separation distance to an outdoor user. Therefore, only the femtocells close to the outdoor user should decrease the used subcarriers to reduce the interference. In this situation, the femtocell capacity is C_{sh1}. On the contrary, the femtocells far away from the outdoor user can still use all subcarriers with capacity C_{sh0}. Suppose that the probability that there is an outdoor user around the considered femtocell is p. With the location awareness, the average spectrum efficiency for the shared spectrum allocation scheme can increase to

$$\text{SE}_{\text{LA}} = \frac{pC_{\text{sh1}} + (1-p)C_{\text{sh0}}}{B}. \tag{9}$$

The existence probability p of an outdoor user around a femtocell can be measured by the femtocell [16] from the long-term statistics depending on the population density, femtocell density, femtocell transmission power, and so on.

To achieve higher spectrum efficiency, the location-aware femtocell system need to adaptively operate in the suitable spectrum allocation scheme and access method according to the existence probability p of an outdoor user and the probability threshold p^*. The probability threshold p^* for selecting the spectrum sharing scheme can be obtained as follows, since SE_{LA} is the average spectrum efficiency for a location-aware femtocell system, as defined in (9). In the condition that using the shared spectrum scheme in the location-aware femtocell system can have higher spectrum efficiency than using the exclusive spectrum scheme, we have

$$\text{SE}_{\text{LA}} = \frac{pC_{\text{sh1}} + (1-p)C_{\text{sh0}}}{B} \geq \text{SE}_{\text{ex}} = \frac{C_{\text{ex}}}{B}. \tag{10}$$

Then, by rearranging (10), we can find the probability threshold p^* as

$$p \leq p^* = \frac{C_{\text{sh0}} - \frac{1}{2}C_{\text{ex}}}{C_{\text{sh0}} - C_{\text{sh1}}}. \tag{11}$$

Accordingly, for the location-aware femtocell system, the shared spectrum allocation scheme can achieve higher spectrum efficiency than the exclusive spectrum allocation scheme as $p < p^*$. The location-aware femtocell need to periodically report the existence probability of outdoor users to the femtocell gateway at the network center. Then, femtocell gateway can calculate the probability threshold by (11) in advance, and adaptively instruct the location-aware femtocells to switch the suitable spectrum allocation and access method. For a given environment, the location-aware femtocells can operate in the shared spectrum allocation scheme if $p < p^*$. Otherwise, the location-aware femtocells should work in the exclusive spectrum allocation scheme to achieve the best spectrum efficiency.

IV. Directional Antennas for Femtocells

Directional antennas can decrease the two-tier interference and thus improve femtocell capacity. For now, most of the fBSs are equipped with only omnidirectional antennas, which have lower antenna gain. In addition, each user will be easily interfered by neighboring femtocells. On the contrary, directional antennas can reduce the interference to adjacent femtocells and achieve the better CINR due to high main lobe gain and narrow beam pattern. In this section, we compare the four-sector switched-beam antenna and the IEEE 802.16m sector antenna.

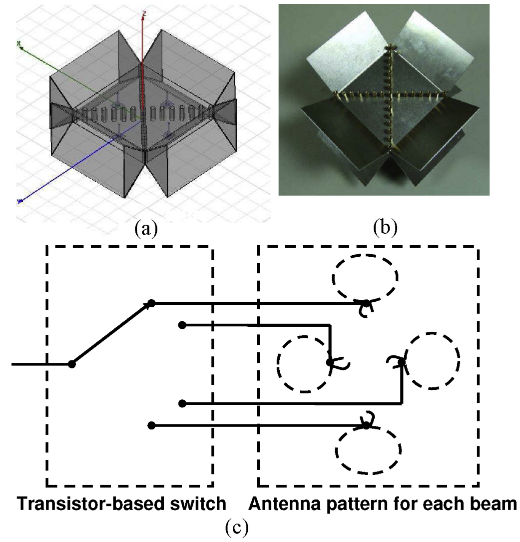

Fig. 3. (a) Structure of four-sector switched-beam directional antenna. (b) Structure of the prototype. (c) Circuitry for the four-sector switched-beam directional antenna with the transistor-based switch.

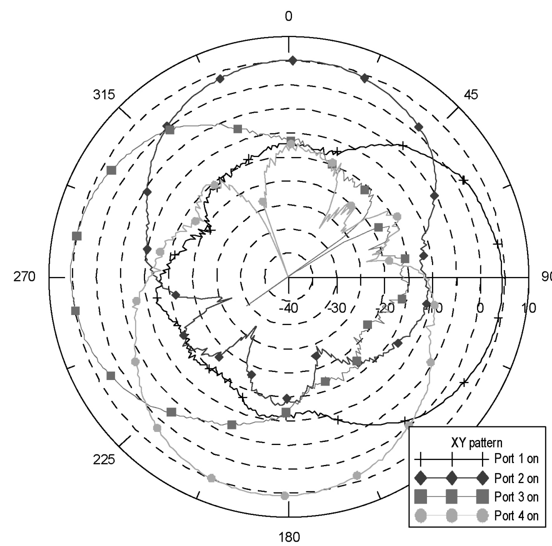

Fig. 4. Each beam pattern of four-sector switched-beam directional antenna.

A. IEEE 802.16m Sector Antenna

We consider the sector antenna in the IEEE 802.16m system [26] which has the radiation pattern $A(\theta)$ as follows:

$$A(\theta) = -\min[12\left(\frac{\theta}{\theta_{3\,\text{dB}}}\right)^2, A_m] \qquad (\text{dB}) \tag{12}$$

where $\theta_{3\,\text{dB}}$ is the 3 dB beamwidth (corresponding to $\theta = 70°$), and $A_m = 20\,\text{dB}$ is the maximum attenuation. The sector antenna pattern in the IEEE 802.16m is mainly designed for outdoor environments. We consider a four-sector fBS that follows the above antenna pattern. Such a four-sector femtocell requires four radio transceivers, yielding higher implementation cost.

B. Four-Sector Switched-Beam Directional Antenna

To resolve the high implementation cost issue of the four-sector femtocell using the IEEE 802.16m sector antenna,

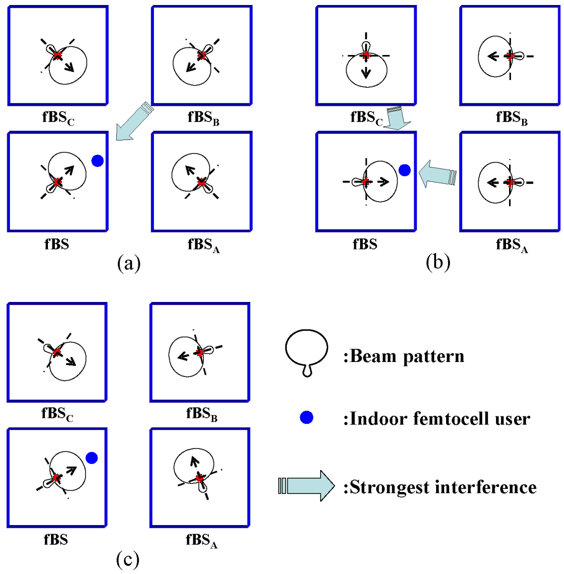

Fig. 5. Effects of antenna azimuth on the interference. (a) Case I. (b) Case II. (c) Case III.

we designed a low-cost E-plane horns-based reconfigurable directional antennas, which required only one single radio transceiver by adopting the switched-beam antenna techniques. Next, we detail the structure of the switched-beam antenna as follows. Fig. 3 shows the structure and prototype of the reconfigurable four-sector switched-beam antenna. This antenna system consists of a transistor-based switch, and post-wall E-plane horns. According to the location of the femtocell user, the switched-beam antenna dynamically alters the beam pattern to the desired user. The low-cost switched-beam antenna needs only one radio transceiver. The beam pattern is shown in Fig. 4. Due to the excellent isolation among E-plane horns, this antenna system also has very low side-lobe level. The size of this antenna prototype is about $19.2 \times 19.2 \times 9.5\,\text{cm}$, which can be downsized further for femtocell applications.

C. Effects of Antenna Azimuth on Interference

The azimuth of directional antenna of the neighboring home base station remarkably affects the interference of a user. If a user is within the main lobe of the neighboring femtocell's antenna, the user suffers from a strong interference. We explain the effects of antenna azimuth on the interference by the example in Fig. 5. In Case I, the main interference of the considered user comes from the neighboring femtocell fBS_B as shown in Fig. 5(a). In Case II [Fig. 5(b)], the neighboring femtocell fBS_A has a strong interference to the considered user. Obviously, compared with Case I, the user in Case II has a higher interference due to a shorter propagation distance. Fig. 5(c) shows the random antenna azimuth case. In practice, the users arbitrarily deploy the fBSs without coordination. Hence, the home base stations have random antenna azimuths. We consider three antenna azimuth cases as shown in Fig. 5(a)–(c) to investigate the effects of azimuth on the link reliability of femtocells.

V. Simulation Results

In this section, we show performance improvements of integrating directional antennas, location awareness, and subcarrier usage ratio adjustment for the OFDMA femtocell systems subject to the femto-to-macro, macro-to-femto, and femto-to-femto interference. We compare our designed four-sector switched-beam antenna with the IEEE 802.16m sector antenna and the 0-dB omnidirectional antenna in both the exclusive and shared spectrum allocation schemes. Macrocells and femtocells in the exclusive spectrum allocation scheme are allocated with nonoverlapping 5 MHz frequency bands. In the shared spectrum allocation scheme, femtocells and macrocells share the total 10 MHz frequency band. We assume that the macrocell system is fully loaded, i.e., all the subcarriers are occupied by the macrocell users. In the meanwhile, it is assumed that macrocell users request one subchannel (i.e., 18 subcarriers) for voice calls. In this fully loaded situation, all the femtocells are interfered by the macrocell system.

Our simulation environment is shown in Fig. 1, where there are 25 femtocells separated by $d_{\text{sf}} = 20\,\text{m}$. These are also covered by a macrocell with a radius of $R_m = 500\,\text{m}$, and the mBS's transmission power is $\widehat{P}_t = 20\,\text{dBm}$. Each fBS is deployed at the center of each house with a shift of (0.1 m, 0.1 m), and all fBSs have the same transmission power $\widetilde{P}_t = 20\,\text{dBm}$. The indoor femtocell users are uniformly distributed within the house. The outdoor users are uniformly located in the shadowed region with width of $(d_{\text{sf}} - 10)/2 = 5\,\text{m}$ surrounding the house, as shown in Fig. 1(b). The channel models and the performance metrics are described in Sections II-C and III, respectively. All results are simulated by MATLAB. Table II [27] lists the related system parameters for the considered OFDMA-based femtocell, including the predefined effective CINR threshold $\gamma_{\text{th}} = -2.5\,\text{dB}$ and link reliability requirement $P_{\text{rel}} = 90\%$. In the OFDMA-based femtocell systems, the more the OFDMA subcarriers used by a femtocell, the higher the femto-to-femto and femto-to-macro interference. Thus, appropriately adjusting the number of used subcarriers can lower the interference. The total number of OFDMA subcarriers for the use of data payload is $N_{\text{ds}} = 720$. Denote N_d as the used subcarriers and define the subcarrier usage ratio as $\rho = \dfrac{N_d}{N_{\text{ds}}}$.

A. Impact of Directional Antenna on Link Reliability

Fig. 6 shows the link reliability performance of indoor femtocell users against the subcarrier usage ratio ρ using the pattern of the switched-beam directional antenna, the IEEE 802.16m sector antenna, and the omnidirectional antenna in both the exclusive and shared spectrum allocation schemes. From the figure, we have the following observations.

1) In the shared spectrum scheme, the switched-beam directional antenna has the best indoor user's link reliability performance because of better capability to overcome the femto-to-femto intercell interference and higher antenna gain. Note that a higher subcarrier usage ratio ρ yields higher femto-to-femto interference. The sector antenna pattern specified in the IEEE 802.16m outperforms the omnidirectional antenna pattern when

TABLE II
OFDMA-BASED FEMTOCELL SYSTEM PARAMETERS

Downlink OFDMA Parameters	Values
Carrier frequency	2.5 GHz
mBS transmit power	43 dBm
fBS transmit power	20 dBm
mBS antenna gain $G(\theta)$	8 dB
Macrocell radius (R_m)	500 m
Noise figure (mBS/fBS/MS)	5 dB/5 dB/7 dB
System bandwidth (B)	10 MHz
Sampling frequency	11.2 MHz
FFT size (M)	1024
Subcarrier bandwidth	10.9375 kHz
Null subcarriers	184
Pilot subcarriers	120
Data subcarriers (N_{ds})	720
Guard fraction (G)	1/8
Predefined effective CINR threshold for link reliability (γ_{th})	−2.5 dB
Minimum link reliability requirement	$P_{\text{rel}} = 90\%$

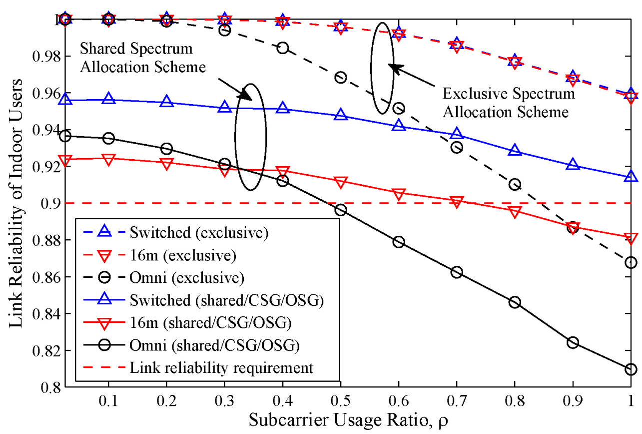

Fig. 6. Link reliability of indoor femtocell user versus the subcarrier usage ratio ρ of the femtocells, for the exclusive and shared spectrum allocation schemes. The switched-beam directional antenna, IEEE 802.16m sector antenna, and 0-dB omnidirectional antenna are compared.

the subcarrier usage ratio $\rho > 0.33$. The directivity of the IEEE 802.16m sector antenna can help reduce the femto-to-femto intercell interference at the range of large value of ρ. For $\rho < 0.33$, however, the IEEE 802.16m sector antenna has worse indoor user's link reliability than the omnidirectional antenna because its antenna gain $A(\theta) < 0$ dB in the azimuth angle $\theta \neq 0^o$ [referring to (12)] and the gain of the omnidirectional antenna is equal to 0 dB in all azimuth angle.

2) Compared with the shared spectrum allocation scheme, the exclusive spectrum allocation scheme has better indoor user's link reliability performance because the macro-to-femto cross-tier interference does not exist. In such a femto-to-femto interference-limited case, the switched-beam directional antenna even with the higher antenna gain yields the similar indoor user's link performance as the IEEE 802.16m sector antenna. Nevertheless, both the switched-beam antenna and the IEEE 802.16m sector antenna perform better than the omnidirectional case.

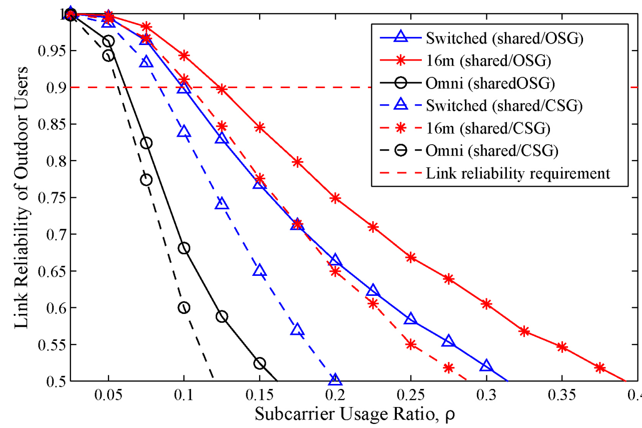

Fig. 7. Link reliability of outdoor user versus the subcarrier usage ratio ρ of the femtocells, in the shared spectrum allocation scheme with the CSG and OSG access methods.

3) To provide high subcarrier usage ratio in femtocell systems, it is important to control the femto-to-femto interference. For the link reliability requirement $P_{\text{rel}} = 90\%$, the switched-beam antenna can support $\rho = 1$ in both shared and exclusive spectrum allocation scheme. However, the IEEE 802.16m sector antenna can support subcarrier usage ratio $\rho = 1$ in the exclusive spectrum allocation scheme, but can only support $\rho = 0.73$ at most in the shared spectrum allocation scheme. For omnidirectional antenna scheme, the largest permissible subcarrier usage ratio $\rho = 0.85$ and $\rho = 0.48$ in the exclusive and shared spectrum allocation schemes, respectively.

Fig. 7 shows the link reliability performance of outdoor user against the subcarrier usage ratio ρ of the femtocells, in the shared spectrum allocation scheme with the CSG and OSG access methods. We assume that in the CSG method the outdoor user around the considered femtocell is served by the macrocell, while the outdoor users can select the base station with the stronger signal strength among the mBS and the fBSs in the OSG method. Besides, the outdoor user needs only one subchannel for voice calls. We have the following observations.

1) The IEEE 802.16m sector antenna can yield better link reliability of outdoor user than the switched-beam antenna for both CSG and OSG methods. Though the higher-gain switched-beam antenna enhances the signal strength, it also increases the interference from femtocells to lower the link reliability of the outdoor user. Nevertheless, both the switched-beam antenna and the IEEE 802.16m sector antenna perform better than the omnidirectional case.

2) To ensure the link reliability of the outdoor users, it is also important to control the femto-to-macro and femto-to-femto interference in the shared spectrum allocation scheme. For the link reliability requirement $P_{\text{rel}} = 90\%$, the IEEE 802.16m sector antenna can support subcarrier usage ratio $\rho = 0.12$ at most in the OSG method, and $\rho = 0.11$ at most in the CSG method. However, the switched-

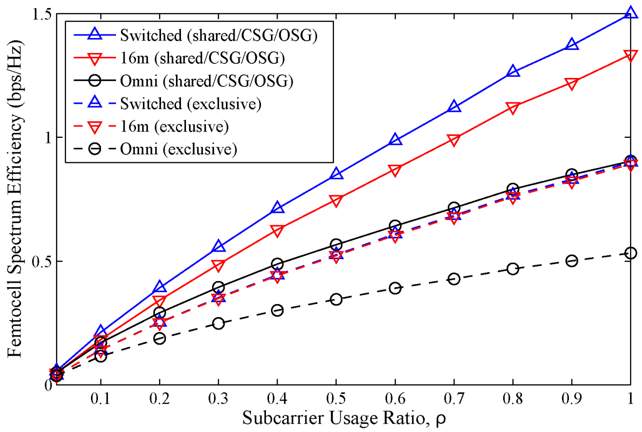

Fig. 8. Femtocell spectrum efficiency versus the subcarrier usage ratio ρ, for the exclusive and shared spectrum allocation schemes with the CSG and OSG access methods.

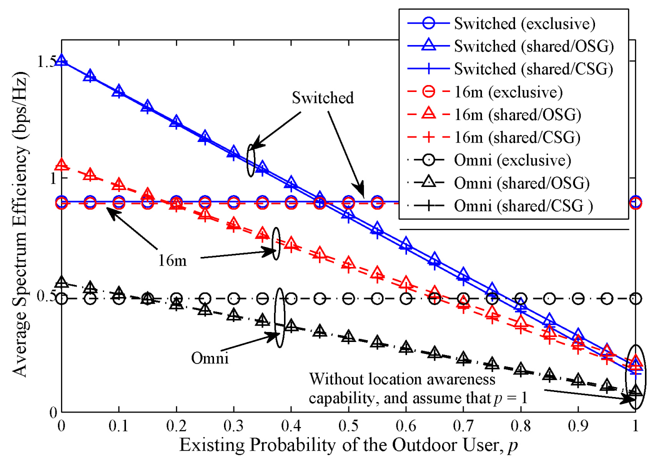

Fig. 9. Average spectrum efficiency of the location-aware femtocell systems versus the existing probability of the outdoor user, under the link reliability requirement $P_{\text{rel}} \geq 90\%$.

beam antenna can support subcarrier usage ratio $\rho = 0.10$ at most in the OSG method, and $\rho = 0.09$ at most in the CSG method. For omnidirectional antenna scheme, the largest permissible subcarrier usage ratio $\rho = 0.065$ and $\rho = 0.06$ in the OSG and CSG methods, respectively.

Fig. 8 shows the spectrum efficiency against the subcarrier usage ratio ρ, for the femtocells with the exclusive and shared spectrum allocation schemes. We have the following observations.

1) It is shown that as the OSG access method and the switched-beam antenna are used to reduce the interference in the shared spectrum scheme, the spectrum efficiency compared with the omnidirectional antenna with the CSG access method is improved from 0.11 b/s/Hz at $\rho = 0.06$ to 0.21 b/s/Hz at $\rho = 0.1$. Therefore, the switched-beam antenna with the OSG method can improve 91% spectrum efficiency compared with the omnidirectional antenna with the CSG method.
2) With a link reliability requirement, the shared spectrum allocation scheme may not always have better spectrum efficiency, even if the macrocells and femtocells share the same spectrum. As far as the switched-beam antenna with link reliability requirement $P_{\text{rel}} = 90\%$ is concerned, the maximum allowable subcarrier usage ratio $\rho = 1.0$ in the exclusive spectrum allocation scheme, and $\rho = 0.1$ in the shared spectrum allocation scheme with the OSG method. The corresponding spectrum efficiency is 0.9 b/s/Hz and 0.21 b/s/Hz in the exclusive spectrum allocation scheme and in the shared spectrum allocation scheme with the OSG method, respectively.
3) It is also shown that with a link reliability requirement, the improvement of the spectrum efficiency is higher than that of the largest permissible subcarrier usage ratio. Compared with the omnidirectional antenna, the directional antenna can improve the link reliability of indoor users to increase the largest permissible subcarrier usage ratio, and thereby improve the spectrum efficiency. As far as the link reliability of indoor users is concerned, in the shared spectrum allocation scheme, the switched-beam antenna can support the largest permissible subcarrier usage ratio $\rho = 1.0$ and achieve 1.5 b/s/Hz spectrum efficiency, while the omnidirectional antenna can support $\rho = 0.48$ and achieve 0.55 b/s/Hz spectrum efficiency. Therefore, the switched-beam antenna can not only improve 108% maximum allowable subcarrier usage ratio but also improve 173% spectrum efficiency, compared with the omnidirectional antenna.

B. Impact of Location Awareness on Spectrum Efficiency

Fig. 9 shows the average spectrum efficiency of the location-aware femtocell systems against the existing probability p of a nearby outdoor user. We assume that if there is an outdoor user around the considered femtocell (referring to Fig. 1), the considered femtocell and all 24 neighboring femtocells should use fewer subcarriers to reduce the interference for this outdoor user. We have the following observations.

1) If the location awareness capability is not available, it is usually assumed that an outdoor user will appear with probability $p = 1$ and thus the maximum allowable subcarrier ratio for femtocell can be set up to $\rho = 0.1$. When the OSG and CSG shared spectrum scheme is used and $p = 1$, the femtocell can achieve spectrum efficiency about 0.2 b/s/Hz for the switched-beam and the IEEE 802.16m sector antennas, but has only 0.1 b/s/Hz for omnidirectional antenna. However, when the femtocell can be aware of the appearance of the outdoor user under the condition $p = 0.4$, the spectrum efficiency can be improved to 1.0 b/s/Hz, 0.7 b/s/Hz, and 0.38 b/s/Hz for the switched-beam antenna, the IEEE 802.16m sector antenna, and omnidirectional antenna, respectively. It implies that location awareness can improve the spectrum efficiency of femtocells by at least two times for different antenna patterns.
2) If the exclusive spectrum allocation scheme is used, location awareness cannot help resolve the interference between femtocells and macrocells, resulting in the same spectrum efficiency for different appearance probabilities of macrocell users.

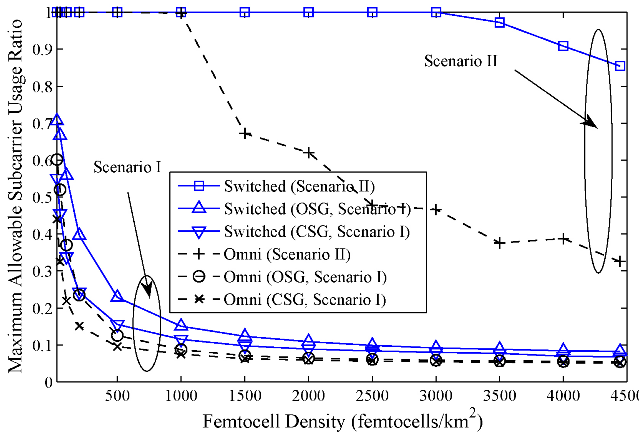

Fig. 10. Maximum allowable subcarrier usage ratio of the location-aware femtocell versus the femtocell density in the shared spectrum allocation scheme subject to the link reliability requirement $P_{\text{rel}} \geq 90\%$. Scenario I: an outdoor user appears near the considered central femtocll. Scenario II: there is no outdoor user around the considered central femtrocell.

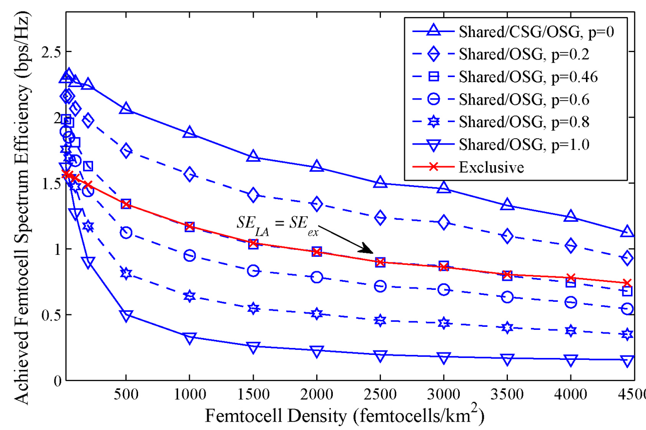

Fig. 11. Achieved spectrum efficiency of the location-aware femtocell versus the femtocell density for different existing probability of an outdoor user under the link reliability requirement $P_{\text{rel}} = 90\%$ in the shared spectrum allocation scheme, where the switched-beam antenna is used.

3) One can observe that location awareness capability can also affect the choice of spectrum sharing schemes for different antenna patterns. When the switched-beam antenna is used, the shared spectrum schemes provide higher spectrum efficiency than the exclusive scheme when $p < 0.46$. The shared spectrum schemes can result in higher spectrum efficiency than the exclusive spectrum scheme only for $p < 0.19$ when the IEEE 802.16m sector antenna is used and for $p < 0.15$ when the omnidirectional antenna is used, respectively.

C. Impacts of Femtocell Density and Existing Probability of Outdoor Users on Spectrum Efficiency

Fig. 10 shows the impact of femtocell density on the maximum allowable subcarrier usage ratio ρ for the location-aware femtocells with the shared spectrum location scheme subject to the link reliability requirement $P_{\text{rel}} \geq 90\%$. We consider two scenarios. Scenarios I represents the situation that an outdoor user appears near the considered central femtocell, and Scenario II represents the situation that an outdoor user does not appear near the considered central femtocell. From the figure, we have the following observations.

1) In Scenario I, the femtocell density significantly affects the maximum allowable subcarrier usage ratio ρ when an outdoor user appears near the considered central femtocell. When the femtocell density is higher than 500 femtocells/km^2 (the corresponding nearest separation distance between two femtocells is $d_{\text{sf}} \approx 45$ m), the maximum allowable subcarrier usage ratio ρ shall be smaller than 0.25 to ensure the link reliability of outdoor users.
2) In Scenario II, the maximum allowable subcarrier usage ratio ρ can be increased since the outdoor user does not exist. For example, when the femtocell density reaches 4500 femtocells/km^2 (the corresponding nearest separation distance between two femtocells is $d_{\text{sf}} \approx 15$ m), a location-aware femtocell system has the potential to improve $\rho = 0.05$ to $\rho = 0.33$ even with omnidirectional antenna. If the switched-beam antenna is used, a location-aware femtocell system has the potential to improve $\rho = 0.08$ to $\rho = 0.85$.

Fig. 11 shows the achieved spectrum efficiency of the location-aware femtocells against the femtocell density for various existing probability p of an outdoor user near the considered femtocell. We consider the location-aware femtocell using the switched-beam antenna and the OSG access method with $P_{\text{rel}} \geq 90\%$ in the shared spectrum allocation scheme. We have the following observations.

1) The existing probability p of an outdoor user significantly affects the achieved spectrum efficiency of the location-aware femtocell system in the shared spectrum allocation scheme. The higher the existing probability p, the lower the achieved spectrum efficiency of the location-aware femtocell system. In this case, if the femtocell density is 1000 femtocells/km^2, the achieved spectrum efficiency of $p = 0$, 0.2, 0.46, 0.6, and 0.8 can be improved by 470%, 373%, 255%, 188%, and 94% compared to that of $p = 1.0$. If the femtocell density is 4000 femtocells/km^2, the spectrum efficiency can be improved by 675%, 544%, 369%, 269%, and 138% for $p = 0$, 0.2, 0.46, 0.6, and 0.8.
2) For the exclusive spectrum allocation scheme with a given femtocell density, the achieved femtocell spectrum efficiency does not fluctuate according to the existing probability p of an outdoor user. This is because the femtocell and macrocell systems are allocated with different frequency bands. For instance, the achieved spectrum efficiency in the exclusive spectrum scheme is 1.2 b/s/Hz and 0.8 b/s/Hz for the femtocell density of 1000 and 4000 femtocells/km^2, respectively.
3) With the information of the existing probability p of a nearby outdoor user and the femtocell density, the location-aware femtocell system can properly choose the spectrum allocation scheme to achieve a better spectrum efficiency. From (11), one can calculate the probability threshold p^* for any given femtocell density. For example, the probability threshold is $p^* = 0.46$ when

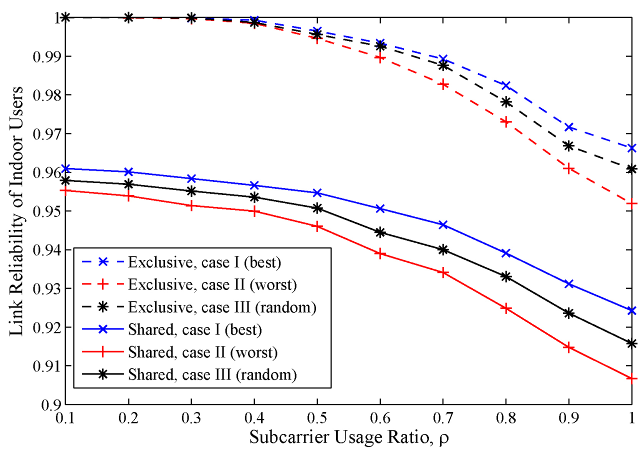

Fig. 12. Link reliability of indoor users versus the subcarrier usage ratio ρ of the femtocells, considering three antenna azimuth cases for the switched-beam antenna.

the femtocell density is 2500 femtocells/km^2. If the existing probability of a nearby outdoor user $p > p^*$, the femtocell system should adopt the exclusive spectrum allocation scheme to achieve a higher spectrum efficiency. If $p \leq p^*$, the location-aware femtocell system can select the shared spectrum scheme to improve the spectrum efficiency.

D. Impact of Antenna Azimuth of Femtocells on Link Reliability

Fig. 12 shows the link reliability of the indoor femtocell users against the subcarrier usage ratio ρ. We consider three antenna azimuth scenarios of the switched-beam femtocells in Fig. 5. However, in this example, the largest difference in link reliability among the three considered cases is only 2.3%. This result implies that the antenna azimuth of switched-beam femtocell has insignificant effects on the link reliability of the femtocell users. Thus, it is implied that femtocells can be deployed with random antenna azimuth.

E. Summary

The proposed design principle aims to help decide the suitable spectrum allocation and access method for femtocells. Actually, without location awareness, it is usually assumed that the existing probability of outdoor user is $p = 1$. In this situation, to guarantee the link reliability of all indoor and outdoor users, the conventional femtocell can only use fewer subcarriers in the shared spectrum allocation scheme or can operate in the exclusive spectrum allocation to alleviate the interference to the other users. Neither the shared spectrum allocation scheme nor the exclusive spectrum allocation scheme is a good option for the conventional femtocell system. On the one hand, spectrum efficiency is too low even if the directional antennas are used to mitigate the interference to the outdoor users in the shared spectrum allocation scheme. On the other hand, the cost for the two times of bandwidth in the exclusive spectrum allocation scheme is too high. On the contrary, if location awareness is available, the shared spectrum allocation scheme can achieve higher spectrum efficiency than the exclusive spectrum allocation scheme as the existing probability of

TABLE III
COMPARISON OF VARIOUS ANTENNA FOR LOCATION-AWARE FEMTOCELLS

Antenna Category	Average Spectrum Efficiency (b/s/Hz) of the Location-Aware Femtocell					
	Spectrum Allocation Schemes and Access Methods	Dense Urban Areas ($p = 0.70$)	Urban Areas ($p = 0.33$)	Suburban Areas ($p = 0.18$)	Rural Areas ($p = 0.04$)	Wilderness ($p = 0.01$)
Switched	Shared/OSG	0.59	1.07 (Best)	1.27 (Best)	1.45 (Best)	1.49 (Best)
	Shared/CSG	0.56	1.06	1.26	1.44	1.48
	Exclusive	0.9 (Best)	0.9	0.9	0.9	0.9
16m	Shared/OSG	0.47	0.78	0.90	1.02	1.04
	Shared/CSG	044	0.77	0.89	1.02	1.04
	Exclusive	0.89	0.89	0.89	0.89	0.89
Omni	Shared/OSG	0.22	0.40	0.47	1.53	0.55
	Shared/CSG	0.22	0.40	0.47	1.53	0.55
	Exclusive	0.48	0.48	0.48	0.48	0.48

The population densities are 3000, 1000, 500, 100, and 25 citizens/km^2 in the dense urban areas, urban areas, suburban areas, rural areas, and wilderness of Europe, respectively [28].

outdoor users is smaller than the probability threshold. The probability threshold can be calculated by (11) in this paper, and the existing probability of outdoor users is decided by the environment.

For a given environment, the location-aware femtocells can operate in the shared spectrum allocation scheme if the existing probability of outdoor users is smaller than the probability threshold, or the location-aware femtocells should work in the exclusive spectrum allocation scheme to achieve better spectrum efficiency. In our example, when the switched-beam antenna is used, the shared spectrum scheme can provide higher spectrum efficiency than the exclusive scheme when the existing probability of outdoor user is $p < 0.46$. We also take some practical environments into account as example. First, according to [28], the population densities in Europe are 3000, 1000, 500, 100, and 25 citizens/km^2 in the dense urban areas, urban areas, suburban areas, rural areas, and wilderness, respectively. In addition, the document [28] also showed that only 8% of the voice calls originate in the busy/peak hour in case the whole population are voice users. In [2], [4], [19], it was mentioned that 50% of all voice calls and 70% of data traffic occur indoors. In other words, only 50% of all voice calls originate outdoors. When the femtocell density is 2500 femtocells/km^2, the region where the cluster of 25 femtocells covers is 0.01 km^2. The probability p_x that there is not any active outdoor voice user in the region is

$$p_x = \left(1 - (0.1)^2\right)^{(D_p \times 0.08 \times 0.5)} \quad (13)$$

where D_p is the corresponding population density. Therefore, the existing probability of outdoor users is the probability that there is at least one outdoor user exists in the region is

$$p = 1 - p_x = 1 - \left(1 - (0.1)^2\right)^{(D_p \times 0.08 \times 0.5)}. \quad (14)$$

Finally, we can determinate that the existing probability of outdoor users are $p = 0.70$, $p = 0.33$, $p = 0.18$, $p = 0.04$, and $p = 0.01$ for the dense urban areas, urban areas, suburban areas, rural areas, and wilderness, respectively.

Table III shows the comparison of various antennas for location-aware femtocells in terms of the average spectrum efficiency. Five environments are considered in the table, and they are the dense urban areas, urban areas, suburban areas, rural areas, and wilderness of Europe [28], respectively. We make a summary of the data given in the table.

1) It can be seen that the switched-beam antenna has the best spectrum efficiency performance for the location-aware femtocells compared with the IEEE 802.16m and the omnidirectional antennas.
2) To have better average spectrum efficiency performance, the location-aware femtocell with the switched-beam antenna should operate in the exclusive spectrum allocation scheme for the dense urban areas, where the existing probability of outdoor users is $p = 0.70$. However, the location-aware femtocell with the switched-beam antenna can operate in the shared spectrum allocation scheme for the urban areas, suburban areas, rural areas, and wilderness, where the existing probabilities of outdoor users are $p = 0.33$, $p = 0.18$, $p = 0.04$, and $p = 0.01$, respectively.

VI. Conclusion

In this paper, we evaluated the throughput of the OFDMA femtocell system with the directional antenna by applying three techniques to reduce the interference between macrocells and femtocells. First, the low-cost four-sector switched-beam antenna was employed to mitigate the interference because of the narrow-beam pattern. Second, the partial usage of subcarriers approach ensured the link reliability of all users by adjusting the number of OFDMA subcarriers used by a femtocell. Third, the location awareness was applied to the femtocell systems for improving spectrum efficiency. Combining these elements, a location-aware femtocell achieved higher spectrum efficiency than the conventional femtocells using the directional antennas, under the link reliability requirement.

The contributions of this paper are described as follows. First, we provided a useful principle for femtocell network planning to select the appropriate spectrum allocation scheme and access method to improve spectrum efficiency. Second, we found that the location awareness capability was essential to the success of improving the femtocell spectrum efficiency because using the directional antenna was not enough to guarantee the link reliability of all indoor and outdoor users. Third, the impacts of spectrum allocation, access method, femtocell density, and directional antenna on link reliability and spectrum efficiency of OFDMA femtocells were investigated, and had some important observations. For example, we found that the shared spectrum scheme may not always have better spectrum efficiency than the exclusive spectrum scheme under the link reliability requirement.

Future Works: In summary, the design principles provided in this paper can help decide the suitable spectrum allocation and access method for the femtocells. There are some interesting research topics that can be extended from this paper, including multiple-user access and subchannel allocation in switch-beam OFDMA femtocells.

References

[1] H. Claussen, L. T. W. Ho, and L. G. Samuel, “An overview of the femtocell concept,” *Bell Labs Tech. J.*, vol. 13, no. 1, pp. 221–246, 2008.

[2] V. Chandrasekhar and J. G. Andrews, “Femtocell networks: A survey,” *IEEE Commun. Mag.*, vol. 46, no. 9, pp. 59–67, Sep. 2008.

[3] S.-P. Yeh, S. Talwar, S.-C. Lee, and H. Kim, “WiMAX femtocells: A perspective on network architecture, capacity, and coverage,” *IEEE Commun. Mag.*, vol. 46, no. 10, pp. 58–65, Oct. 2008.

[4] D. López-Pérez, A. Valcarce, G. de la Roche, and J. Zhang, “OFDMA femtocells: A roadmap on interference avoidance,” *IEEE Commun. Mag.*, vol. 47, no. 9, pp. 41–48, Sep. 2009.

[5] R. Y. Kim, J. S. Kwak, and K. Etemad, “WiMAX femtocell: Requirements, challenges, and solutions,” *IEEE Commun. Mag.*, vol. 47, no. 9, pp. 84–91, Sep. 2009.

[6] V. Chandrasekhar, J. G. Andrews, T. Muharemovic, Z. Shen, and A. Gatherer, “Power control in two-tier femtocell networks,” *IEEE Trans. Wireless Commun.*, vol. 8, no. 8, pp. 4316–4328, Aug. 2009.

[7] G. de la Roche, A. Valcarce, D. López-Pérez, and J. Zhang, “Access control mechanisms for femtocells,” *IEEE Commun. Mag.*, vol. 48, no. 1, pp. 33–39, Jan. 2010.

[8] P. Xia, V. Chandrasekhar, and J. G. Andrews, “Open vs. closed access femtocell in the uplink,” *IEEE Trans. Wireless Commun.*, vol. 9, no. 12, pp. 3798–3809, Dec. 2010.

[9] H. Zeng, C. Zhu, and W.-P. Chen, “System performance of self-organizing network algorithm in WiMAX femtocells,” in *Proc. Int. WICON*, no. 25. Nov. 2008, pp. 1–9.

[10] V. Chandrasekhar and J. G. Andrews, “Spectrum allocation in tiered cellular networks,” *IEEE Trans. Commun.*, vol. 57, no. 10, pp. 3059–3068, Oct. 2009.

[11] C. Lee, J.-H. Huang, and L.-C. Wang, “Distributed channel selection principles for femtocells with two-tier interference,” in *Proc. IEEE VTC*, May 2010, pp. 1–5.

[12] C.-H. Ko and H.-Y. Wei, “On-demand resource-sharing mechanism design in two-tier OFDMA femtocell networks,” *IEEE Trans. Vehicular Technol.*, vol. 60, no. 3, pp. 1059–1071, Mar. 2011.

[13] S.-Y. Lien, C.-C. Tseng, K.-C. Chen, and C.-W. Su, “Cognitive radio resource management for QoS guarantees in autonomous femtocell networks,” in *Proc. IEEE ICC*, May 2010, pp. 1–6.

[14] S.-Y. Lien, Y.-Y. Lin, and K.-C. Chen, “Cognitive and game-theoretical radio resource management for autonomous femtocells with QoS guarantees,” *IEEE Trans. Wireless Commun.*, vol. 10, no. 7, pp. 2196–2206, Jul. 2011.

[15] V. Chandrasekhar and J. G. Andrews, “Uplink capacity and interference avoidance for two-tier femtocell networks,” *IEEE Trans. Wireless Commun.*, vol. 8, no. 7, pp. 3498–3509, Jul. 2009.

[16] H. Claussen, F. Pivit, and L. T. W. Ho, “Self-optimization of femtocell coverage to minimize the increase in core network mobility signalling,” *Bell Labs Tech. J.*, vol. 14, no. 2, pp. 155–184, 2009.

[17] S.-G. Josep and W. H. Chin, “Performance of an LTE femtocell base station employing uplink antenna selection,” in *Proc. WiAd*, Jun. 2011, pp. 224–229.

[18] N.-D. Dáo, Y. Sun, and W. H. Chin, “Receive antenna selection techniques for femtocell uplink interference mitigation,” in *Proc. IEEE Int. Symp. PIMRC Workshops*, Sep. 2010, pp. 180–184.

[19] Y. Jeong, H. Kim, B.-S. Kim, and H. Choo, “Avoidance of co-channel interference using switched parasitic array antenna in femtocell networks,” in *Proc. ICCSA*, vol. 6018. 2010, pp. 158–167.

[20] A.-H. Tsai, J.-H. Huang, L.-C. Wang, and R.-B. Hwang, “High capacity femtocells with directional antennas,” in *Proc. IEEE WCNC*, Apr. 2010, pp. 1–6.

[21] R. Srinivasan and S. Hamiti, “IEEE 802.16m system description document (SDD),” IEEE 802.16 Broadband Wireless Access Working Group, Tech. Rep. IEEE 802.16m-09/0034r2, Sep. 2009.

[22] V. Erceg, L. Schumacher, P. Kyritsi, A. Molisch, D. S. Baum, A. Y. Gorokhov, C. Oestges, C. Lanzl, V. J. Rhodes, J. Medbo, D. Michelson, M. Webster, E. Jacobsen, D. Cheung, Q. Li, C. Prettie, M. Ho, S. Howard, B. Bjerke, K. Yu, L. Jengx, A. Jagannatham, N. Tal, S. Valle, and A. Poloni, “Indoor MIMO WLAN channel models,” IEEE P802.11 Wireless LANs, Tech. Rep. IEEE 802.11-03/871r1, Nov. 2003.

[23] V. Erceg, K. V. S. Hari, M. S. Smith, D. S. Baum, K. P. Sheikh, C. Tappenden, J. M. Costa, C. Bushue, A. Sarajedini, R. Schwartz, D. Branlund, T. Kaitz, and D. Trinkwon, “Channel models for fixed wireless applications,” IEEE 802.16 Broadband Wireless Access Working Group, Tech. Rep. IEEE 802.16.3c-01/29r4, Jul. 2001.

[24] R. Yaniv, D. Stopler, T. Kaitz, and K. Blum, "CINR measurements using the EESM method," IEEE 802.16 Broadband Wireless Access Working Group, Tech. Rep. IEEE C802.16e-05/141, Mar. 2005.
[25] J. G. Andrews, A. Ghosh, and R. Muhamed, *Fundamentals of WiMAX*. Englewood Cliffs, NJ: Prentice-Hall, 2007.
[26] R. Srinivasan, J. Zhuang, L. Jalloul, R. Novak, and J. Park, "IEEE 802.16 m evaluation methodology document (EMD)," IEEE 802.16 Broadband Wireless Access Working Group, Tech. Rep. IEEE 802.16m-08/004r4, Nov. 2008.
[27] WiMAX Forum, "WiMAX system evaluation methodology," Version 2.1, Jul. 2008.
[28] M. A. Imran, E. Katranaras, G. Auer, O. Blume, V. Giannini, I. Godor, Y. Jading, M. Olsson, D. Sabella, P. Skillermark, and W. Wajda, "Energy efficiency analysis of the reference systems, areas of improvements and target breakdown," Energy Aware Radio and neTwork tecHnologies (EARTH), Tech. Rep. INFSO-ICT-247733 EARTH Deliverable D2.3, Nov. 2010.

Ang-Hsun Tsai (S'09) received the B.S. degree in electrical engineering from the Chung Cheng Institute of Technology, National Defense University, Taoyuan, Taiwan, in 1998, and the M.S. degree in electro-optical engineering from the National Sun Yat-Sen University, Kaohsiung, Taiwan, in 2005. He is currently pursuing the Ph.D. degree from the Department of Electrical Engineering, National Chiao Tung University, Hsinchu, Taiwan.

His current research interests include femtocell networks, heterogeneous machine-type communications networks, and radio resource management.

Mr. Tsai was elected an Honorary Member of the Phi Tau Phi Scholastic Honor Society of the Republic of China by National Sun Yet-Sen University in 2005.

Li-Chun Wang (S'92–M'96–SM'06–F'11) received the B.S. degree from the National Chiao Tung University, Hsinchu, Taiwan, in 1986, the M.S. degree from the National Taiwan University, Taipei, Taiwan, in 1988, and the M.Sc. and Ph.D. degrees from the Georgia Institute of Technology, Atlanta, in 1995 and 1996, respectively, all in electrical engineering.

From 1990 to 1992, he was with the Telecommunications Laboratories of the Ministry of Transportations and Communications in Taiwan (currently, the Telecom Laboratories of Chunghwa Telecom Company, Taipei). In 1995, he was with Bell Northern Research of Northern Telecom, Inc., Richardson, TX. From 1996 to 2000, he was a Senior Technical Staff Member with the Wireless Communications Research Department, AT&T Laboratories, Austin, TX. In August 2000, he became an Associate Professor with the Department of Electrical Engineering, National Chiao Tung University, where he is currently a Full Professor since 2005. He has published over 150 journal and international conference papers. He currently holds nine U.S. patents. His current research interests include radio resource management and cross-layer optimization techniques for wireless systems, heterogeneous wireless network designs, and cloud computing for mobile applications.

Dr. Wang was a co-recipient (with G. L. Stuber and C.-T. Lea) of the 1997 IEEE Jack Neubauer Best Paper Award for his paper "Architecture design, frequency planning, and performance analysis for a microcell/macrocell overlaying system," published in the IEEE TRANSACTIONS ON VEHICULAR TECHNOLOGY (vol. 46, no. 4, pp. 836–848, Nov. 1997). He was an Associate Editor of the IEEE TRANSACTIONS ON WIRELESS COMMUNICATIONS from 2001 to 2005, the Guest Editor of the Special Issue on "Mobile computing and networking" for the IEEE JOURNAL ON SELECTED AREAS IN COMMUNICATIONS in 2005 and "Radio resource management and protocol engineering in future IEEE broadband networks" for the IEEE WIRELESS COMMUNICATIONS MAGAZINE in 2006.

Jane-Hwa Huang (M'09) received the B.S., M.S., and Ph.D. degrees in electrical engineering from the National Cheng Kung University, Tainan, Taiwan, in 1994, 1996, and 2003, respectively.

He joined the Department of Communication Engineering, National Chiao Tung University, Hsinchu, Taiwan, as a Post-Doctoral Researcher from 2004 to January 2006, where he later became a Research Assistant Professor. Since August 2009, he has been an Assistant Professor with the Department of Electrical Engineering, National Chi Nan University, Nantou, Taiwan. His current research interests include wireless networks, green communications, wireless multihop communications, and radio resource management.

Ruey-Bing Hwang (M'96–SM'06) was born in Nantou, Taiwan, on January 20, 1967. He received the B.S. degree in communication engineering and the Ph.D. degree from the Institute of Electronics, National Chiao Tung University, Hsinchu, Taiwan, in 1990 and 1996, respectively.

He is currently a Professor with the Department of Electrical Engineering, National Chiao Tung University. His current research interests include periodic structures, photonic crystals, metamaterials, antenna designs, and electromagnetic compatibility.